

Pose Guidance by Supervision: A Framework for Clothes-Changing Person Re-Identification

Quoc-Huy Trinh^{1,3}, Nhat-Tan Bui^{4*}, Phuoc-Thao Vo Thi^{1,3}, Hai-Dang Nguyen^{1,2,3}, Debesh Jha⁵, Ulas Bagci⁵, and Minh-Triet Tran^{1,2,3}

¹University of Science, VNU-HCM ²John von Neumann Institute, VNU-HCM

³Vietnam National University, Ho Chi Minh City, Vietnam

⁴Department of EECS, University of Arkansas, Fayetteville, Arkansas, USA

⁵Department of Radiology, Northwestern University, Chicago, Illinois, USA

Abstract. Person Re-Identification (ReID) task seeks to enhance the tracking of multiple individuals by surveillance cameras. It provides additional support for multimodal tasks, including text-based person retrieval and human matching. One of the primary challenges in ReID is clothes-changing, which means the same person wears different clothes. While previous methods have achieved competitive results in maintaining clothing data consistency and handling clothing change data, they still tend to rely excessively on clothing information, thus limiting performance due to the dynamic nature of human appearances. To mitigate this challenge, we propose the Pose Guidance by Supervision (PGS) framework, an effective framework for learning pose guidance within the ReID task. This approach leverages pose knowledge and human part information from the pre-trained features to guide the network focus on clothes-irrelevant information, thus alleviating the clothes' influence on the deep learning model. Extensive experiments on five benchmark datasets demonstrate that our framework achieves competitive results compared with other state-of-the-art methods, which holds promise for developing robust models in the ReID task. Our code is available at <https://github.com/huyquoctrinh/PGS>.

Keywords: Person Re-Identification · Pose Guidance · Clothes-Changing

1 Introduction

Person Re-Identification (ReID) is the task of tracking and distinguishing individuals across multiple cameras and viewpoints. The application of this technique is in surveillance camera systems, enabling the search, tracking, and identification of unidentified individuals within a town or specific area, thereby enhancing security measures. With the development of deep learning, several methods have gained prominent performance in the ReID task. Those aforementioned works

* Work done when Nhat-Tan Bui was at the University of Science, VNU-HCM, Vietnam and prior to joining the University of Arkansas, USA.

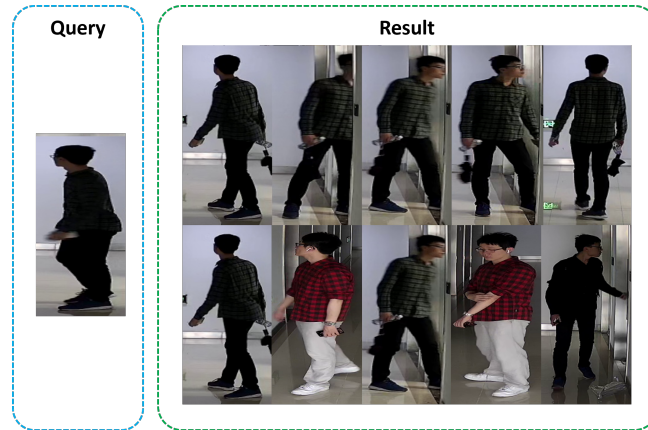


Fig. 1: Illustration of the retrieval result. In the result frame, the first row illustrates the clothes-consistent result, while the second row shows the clothes-changing result.

can be separated into four approaches. Firstly, many studies, such as [7, 14] concentrate on loss function to facilitate improved representation learning. Secondly, architecture-based methods [2, 8] are proposed to enhance feature extraction capabilities. Thirdly, the self-supervised learning frameworks [3, 23, 31] have been designed to facilitate model learning on extensive pedestrian datasets, which contain a substantial amount of unlabelled data. Finally, the multi-modal approaches [6, 16, 30] assist the model in assimilating information from various domains.

Although previous approaches have obtained amazing research progress in ReID, the clothes-changing problem is still a challenge that should be taken into account. This problem is especially critical for real-world applications where people always change their clothes. In recent years, researchers involved in the ReID task are paying more attention to the clothes-changing problem with the appearance of the VC-Clothes [28], and LTCC [25]. The main reason for the difficulty of this challenge is the deep learning model’s reliance on the cloth appearance. This means that the model makes predictions based on what a person is wearing, not on his or her biometric traits (e.g. face, hair, pose, gait). Our insight underscores that the lack of pose information during the learning process tends to be the main reason leading to the clothes-changing problem. Therefore, a promising strategy is focusing on the pose knowledge and human part information, which the pre-trained pose estimation model can extract.

As a result, in this paper, we propose the **P**ose **G**uidance by **S**upervision method (PGS), a simple and innovative framework for the clothes-changing ReID task. As shown in Figure 1, our framework can overcome the challenge of the clothes-changing problem in ReID task. In essence, our method builds upon three main modules: human encoder, pose encoder and Transformer Transfer

Knowledge (TTK) module. The human encoder efficiently adapts SOLIDER [3], a self-supervised learning framework for human-centric tasks, to extract the general human representations from the input images. While the pose encoder is taken from the pose estimation model OpenPose [1] to generate meaningful global features for biometric identification, which includes the pose, body, foot, hand, and facial. Our TTK module operates between two encoders to transfer the pose information extracted from the pose encoder to the human encoder across various scales. This strategy aims to use the body part knowledge to guide the model in the learning stage. In practice, we choose to fine-tune the pre-trained human encoder and train our TTK module while freezing the pose encoder since we only need the general human pose information from the pose encoder. In summary, this paper’s main contributions are:

- We explore the potential of the feature representation from the pose estimation model to overcome the clothes-changing problem. We believe this simple strategy can serve as the baseline approach to alleviate the clothes-changing effect on the ReID task.
- We implement a ReID framework, termed PGS, which involves guiding the model by the pre-trained features from the pose estimation method at various scales to enable the pose knowledge learning process.
- We extensively evaluate our method on five datasets, i.e., Market-1501 [34], DukeMTMC [27], CuHK03 [17, 35], LTCC [25] and VC-Clothes [28].

The content of this paper is organized as follows. In Section 2, we briefly review existing methods for Person Re-Identification as well as Clothes-changing Re-Identification problems. Then we introduce our proposed method in Section 3. The experiments are presented in Section 4. Finally, we conclude our work and suggest problems for future work in Section 5.

2 Related Work

Person Re-Identification: The ReID task involves distinguishing between individuals in surveillance camera footage. Bag of Tricks method [22] serves as the baseline approach for subsequent studies since it provides effective training tricks on this task. Pose-transfer [19] utilizes the human pose instances to create the sample augmentation in new poses to improve the ReID model’s performance. ABDNet [2] integrates two attention modules (e.g., CAM and PAM) with the novel regularization to learn robust feature representation. MNDM [4] method uses the multi-branch network with dynamic matching for the ReID task. TransReID [10] proposes a pure transformer-based network with two novel modules to mitigate the data bias toward various cameras or viewpoints. Auto-ReID+ [8], which is built on the Auto-ReID framework [26], proposes the multi-branch macro network search architecture that combines multi-scale features, local, and global features to benefit the ReID model. PGFL-KD [33] exploits the pose-guided interaction learning to regularize the global feature’s learning. AMSL [7] proposes an adaptive mining sample loss, which allocates weights adaptively

based on the Euclidean distance between samples. AML [14] designs an adaptive multiple loss baseline on the base of triple loss to avoid the misjudgment of samples.

Clothes-changing Re-Identification: The introduction of the LTCC datasets [25] marked a significant development to address the clothes-changing problem. After that, FSAM [13] aims to get the coarse ID masks with structure-related details, incorporating ID-relevant information for discriminative structural feature extraction. CAL [9] proposes a novel multi-positive-class classification loss to formulate multi-class adversarial learning. GI-ReID [15] integrates the clothes classification and the casual inference model for mitigating the bias on the clothes information. AIM [32] defines a causality-based Auto Intervention Model to mitigate clothing bias for the robust cloth-changing person. FIRE² [29] introduces the fine-grained feature mining and fine-grained attribute recombination module to boost the learning of robust features. Although previous works achieved impressive results on the clothes changing task, it is worth noting that these methods lack focusing on the crucial part of the body, which is the salient information to distinguish a specific person.

From the above analysis, as a consequence, we design PGS to concentrate to the body part information. Thereby, the model can effectively utilize information from different body regions, including the head, arms, legs, and upper body, to distinguish and identify individuals. This approach helps reduce the model’s dependence on clothing-related information. Moreover, integrating the pre-trained pose estimation model also avoids the increase of the computation cost in the inference stage.

3 Proposed PGS

In this section, we will introduce our PGS framework, which comprises three main modules: a human encoder, a pose encoder, and a TTK (Transformer Transfer Knowledge) module. Unlike Pose-transfer [19] and PGFL-KD [33], instead of designing complex modules to obtain body part features, our method leverages the pre-trained features from a pose estimation model in a simple fashion, as depicted in Figure 2. The human encoder learns the feature representations and unique gait of each person, while the pose encoder (i.e., from pre-trained model) is used to extract the human pose information from the input image.

Most existing ReID methods often suffer the problem of clothes-changing, as they distinguish different IDs (i.e. people) by the clothes. Recognizing the importance of body pose and human body information (e.g. face, hair, pose, gait), we propose a Transformer Transfer Knowledge module (TTK) that operates between each block of the encoder. In short, TTK’s goal is to transfer knowledge from the pre-trained features of the pose estimation model to the main ReID model. We detail each component in the following section.

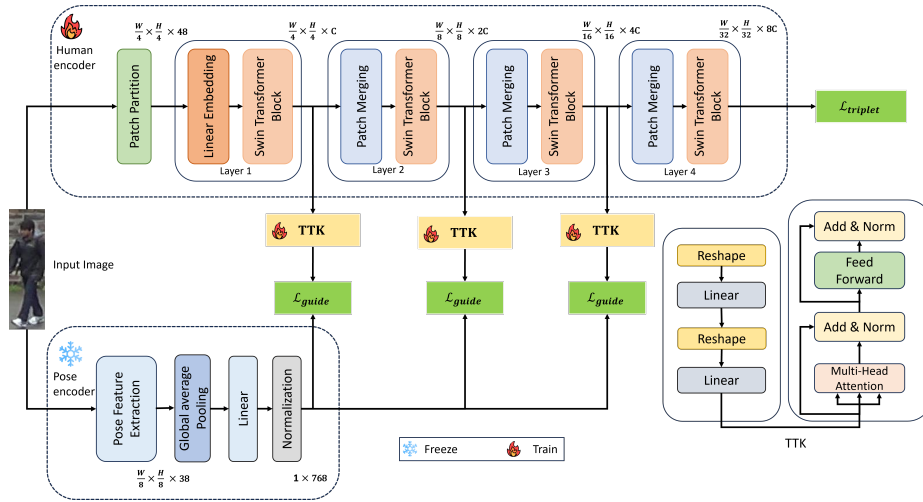


Fig. 2: Overall framework of proposed PGS, including three parts, i.e., *human encoder* and *pose encoder*, which leverages pre-trained features to extract general human representations, and the novel *Transformer Transfer Knowledge (TTK)* module, designed to effectively transfer biometric trait knowledge from the pose encoder to the human encoder. Here, H, W , and C denote the height, width, and channel, respectively. Similarly, $\mathcal{L}_{triplet}$ is the triplet loss [12] which aids in acquiring person-centric representations and \mathcal{L}_{guide} is the guide loss to transfer the pose knowledge from the pose encoder to the human encoder.

3.1 Human Encoder

Our human encoder is derived from the student network of SOLIDER [3], a human-centric self-supervised learning framework, without any modification. We assume the bases of SOLIDER’s parameter space are capable of applying to diverse downstream human-centric tasks, including ReID, due to its meaningful semantic representation. Thus, it is plausible to fine-tune the SOLIDER’s original parameter space to attain rich human semantic representation, which is salient information to distinguish different people. It is important to note that the model’s performance could potentially be enhanced through an exhaustive search for appropriate pre-trained features.

The backbone for the human encoder is the Swin Transformer [20], which consists of four main layers. Given an input human image $X \in \mathbb{R}^{W \times H \times 3}$ where W, H represents the width and height of the image and 3 identifies the number of channels. After four layers, the human backbone will encode the images into the embedding $f^h \in \mathbb{R}^{1 \times 768}$. This image embedding will be sent through the fully connected layer to produce the final result. Additionally, this image embedding also serves as the input for the triplet loss function [12], which we will detail in the following section.

3.2 Pose Encoder

As mentioned before, the proposed PGS aims to transfer the biometric information (e.g., gait, pose, body, foot, hand, and hair) to consolidate the model’s capacity to identify the same person wearing different clothes. Thus, we propose a simple strategy that exploits a pre-trained pose estimation to enhance the ReID model’s ability to concentrate on body part information instead of cloth appearance.

Our pose encoder is based on the encoder from the OpenPose [1], a popular 2D pose estimation model. We hypothesize that the feature representation from OpenPose is complete enough for our framework since we only want to get the general human part information. As a consequence, we keep the pose encoder unchanged so that we can minimize the number of parameters during training. Similar to the human encoder, the choice of the pre-trained pose estimation representation can significantly affect the overall performance of ReID model.

The pose encoder takes the input human image to generate the confidence map (i.e. pose feature), which presents each part of the human. The confidence map is then passed through the global average pooling and fully connected layer to produce the meaningful feature maps $f^p \in \mathbb{R}^{1 \times 768}$ that are associated with the human parts.

3.3 Transformer Transfer Knowledge Module (TTK)

The primary objective of the TTK module is to robustly transfer human part knowledge from the pose encoder to the human encoder across multiple scales. Our TTK is primarily composed of two stages: reduction and transformation.

In the reduction stage, at i -th layer, the TTK module takes the embedding feature $f_i^h \in \mathbb{R}^{H_i \times W_i \times C_i}$ from the human encoder to produce the feature map $f_i^r \in \mathbb{R}^{16 \times 768}$. This stage consists of 2 fully connected layers. Specifically, we first reshape the embedding feature f_i^h into a 2D matrix of size $(H \times W) \times C$. Then, these features are passed through the first fully connected layer to reduce the number of channels to 16, thus generating the f_i^r feature map of size $(H \times W) \times 16$. Again, we reshape the f_i^r feature map to get the size of $16 \times (H \times W)$. Finally, for the purpose of reducing the number of parameters, we subject the reduction feature f_i^r to the second fully connected layer to yield the final reduction feature, i.e., $f_i^r \in \mathbb{R}^{16 \times 768}$.

In the transformation stage, we utilize the Transformer layer, which builds upon the concept of ViT [5] framework. As shown in Figure 2, this stage contains two blocks: multi-head self-attention (MSA) and feed-forward network (FFN). After MSA as well as FFN, layer normalization and residual connection are added, respectively. The reduction feature $f_i^r \in \mathbb{R}^{16 \times 768}$ is the input of this layer. Then, one attention head is calculated as follows:

$$Attention(Q, K, V) = Softmax\left(\frac{QK^T}{\sqrt{d_k}}\right)V \quad (1)$$

where Q, K, V signify queries, keys, and values which can be generated by f_i^r through fully connected layers. $\sqrt{d_k}$ is used to avoid very small gradient values. MSA can be obtained by calculating the group N of attention head, which equals 16 in our experiment. Then, the final output f_i^t is expressed as follows:

$$f_i^{MSA} = LN(MSA(f_i^r)) + f_i^r \quad (2)$$

$$f_i^t = LN(FFN(f_i^{MSA})) + f_i^{MSA} \quad (3)$$

where LN denotes layer normalization and FFN is the fully connected layer. By this simple approach, the TTK module guarantees to transfer the specific information about the biometric traits in the pose encoder to the human encoder without the extra number of parameters.

3.4 Objective Functions

Our framework is trained end-to-end with a combined loss, which is defined as in Equation 4.

$$\mathcal{L}_{combined} = \mathcal{L}_{triplet} + \lambda \mathcal{L}_{guide} \quad (4)$$

where $\mathcal{L}_{triplet}$ is the triple loss [12] to learn person-specific representations, and \mathcal{L}_{guide} is the guide loss to transfer the pose knowledge from pose encoder to human encoder. The hyperparameter λ , which we set to 0.2, is used to control the contribution and effect of the guide loss on the whole system.

Triplet Loss: For the purpose of learning a discriminative embedding in the feature space (i.e., encouraging representations of the same person to be similar to one another), we adapt the popular deep metric learning triplet loss [12], which is defined as follows:

$$\mathcal{L}_{triplet} = \sum_{i=1}^N [\|f_i^a - f_i^p\|_2^2 - \|f_i^a - f_i^n\|_2^2 + \alpha] \quad (5)$$

where N corresponds to the number of data samples in a batch, i denotes the index of the sample, f stands for the embedding from the human encoder, a, p, n symbols individually refer to the anchor, positive, and negative instances. We employ batch hard-triplet mining [11] for the triplet selection. The parameter α signifies the margin, dictating the separation between embeddings. In our work, we set α equals 0.2.

Guide Loss: For the guidance of the pose feature to the human representation feature, we investigate the KL-divergence loss, which is presented in Equation 6.

$$\mathcal{L}_{guide} = \frac{1}{N} \sum_{i=1}^N (f^p \cdot \log(\frac{f^p}{f_i^t})) \quad (6)$$

where N denotes the number of layers, f^p denotes the pose embedding taken from the pose encoder, f_i^t is the human feature map after going through the

TTK module at the i^{th} layer. Before computing the guide loss, both f_p and f_i^t are rescaled by softmax and divided by the temperature, which can be defined as follows:

$$f = \frac{1}{T} \times \frac{e^f}{\sum_{i=1}^N f^i} \quad (7)$$

where T denotes the temperature, which equals 2 in this work; f is represented for the embedding; N corresponds to the number of channels within the embedding, where the index is represented by i .

During the training phase, the primary objective of this loss function is to minimize the disparity between the distributions originating from pose embeddings and human embeddings. This process leads to the identification of optimal weights for refining the learning of both pose and human appearance representations. This, in turn, facilitates the model in grasping both appearance-related information and pose-related knowledge. Since our goal is to introduce a simple framework that can transfer the biometric knowledge to the ReID task, we do not exhaustive search for the best loss functions, which means other researchers can continue to explore the potential of other loss functions in this task.

4 Experiment

4.1 Datasets

We evaluate the proposed PGS on five datasets. **Market-1501** [34] contains 1,501 identities observed from 6 camera viewpoints, including 12,936 training images of 751 identities, 19,732 gallery images, and 2,228 queries. **Duke-MTMC** [27] comprises 34,183 images of 1,404 identities from eight cameras. It contains 16,522 training images, 17,661 gallery images, and 2,228 queries. **CuHK03** [17, 35] contains 14,097 pictures of 1,467 identities. Additionally, the dataset offers 20 different sets for training and testing, where 100 identities are reserved for testing in each set while the remaining identities are used for training. **LTCC** [25] contains 17,119 person images of 152 identities. The training set in this data includes 9,576 images with 77 identities (46 clothes-changing IDs and 31 clothes-consistent IDs). The testing set includes 493 query images and 7,050 test images with 75 identities (45 clothes-changing IDs + 30 clothes-consistent IDs). This dataset includes two types of testing: *Standard* (test cases including clothes-changing and clothes-consistent), and *CC* (test cases include only clothes-changing IDs). **VC-Clothes** [28] comprises synthesized human images. It encompasses a total of 19,060 images of 512 unique identities in four scenes. In the training phase, 9449 images of 256 identities are employed, leaving the remaining 9611 images of 256 identities for the testing phase.

4.2 Implementation Detail

During the training and testing phase, all of the images are resized to dimensions of 384×128 . Our training and testing for the clothes-consistent follow the setting

of Bag of Trick [22], while in the clothes-changing testing, we follow the setup of LTCC [25]. The Pytorch framework is used, and all of the experiments are done on the Tesla A100 40GB GPU. For the hyperparameters, the batch size for the training and testing is 64; we also use the learning rate scheduler to support our training experiments with a base learning rate of $8e-4$, and the temperature value equals 2. We choose the AdamW [21] as our optimizer, and the best weight has been gotten after 250 epochs. For data augmentation, we employ random horizontal flip and random erasing.

4.3 Baselines and Evaluation Metrics

Baselines: Based on two kinds of ReID problems, we select different baselines in two scenarios as follows. For **clothes-consistent** setting, we evaluate our method on Market-1501, Duke-MTMC and CuHK03 datasets. We compare our method with several state-of-the-art methods on the ReID task, including Pose-transfer [19], Bag of Trick [22], ABDNet [2], MNDM [4], AMSL [7], Auto-ReID+ [8], TransReID [10], PGFL-KD [33], AML [14], PFD [30], and SOLIDER [3]. Regarding the SOLIDER baseline, we reproduce the results on the Duke-MTMC dataset and the CuHK03 dataset. For **clothes-changing** setting, we evaluate our method on LTCC-Standard, LTCC-CC and VC-Clothes datasets. For LTCC dataset, we compare our method with other state-of-the-art methods (i.e., LTCC [25], FSAM [13], CAL [9], GI-ReID [15], AIM [32], and FIRE² [29]). Regarding for the testing on the VC-Clothes dataset, we compare our method with the following methods: FSAM [13], GI-ReID [15], and AIM [32].

Evaluation Metrics: To conduct a fair comparison with other methods, we employ two metrics, i.e., mean Average Precision (mAP), and Rank-1 accuracy (R1). mAP is calculated via the area under the precision-recall curve while R1 is defined by how many samples are correct in the top-1 prediction.

4.4 Performance Comparisons

We report the performance of our proposed PGS with three different versions: PGS-1, PGS-2, and PGS-3 which include one to three layers for guidance supervision, respectively. The results for the clothes-consistent setting are shown in Table 1 while the clothes-changing setting are shown in Table 2.

Clothes-consistent: From Table 1, it is evident that our method can lead to an improvement of +0.3% in the mAP metric and +0.6% in the R1 metric. In the CuHK03 dataset, our method outperforms the second-best method by a margin of +6% in the mAP metric and +1.2% in the R1 metric. As for the Duke-MTMC dataset, our method achieves a better mAP metric by +1.0%, and +2.0% in the R1 metric. These results clearly demonstrate that our method is competitive with state-of-the-art approaches across all three datasets, underscoring the effectiveness of leveraging pose information for distinguishing individuals. This outcome is significant in showcasing the potential of our approach for future studies.

Method	Market-1501		Duke-MTMC		CuHK03	
	mAP	R1	MAP	R1	mAP	R1
Pose-transfer [19]	68.9	87.7	56.9	78.5	42.0	45.1
Bag of Trick [22]	94.2	95.4	89.1	90.3	56.6	58.8
ABDNet [2]	88.3	95.6	78.6	89.0	--	--
MNDM [4]	93.0	95.0	86.0	74.4	73.1	76.3
AMSL [7]	88.1	95.1	78.2	89.4	75.6	78.4
Auto-ReID+ [8]	88.2	95.8	80.1	90.1	74.2	78.1
TransReID [10]	89.0	95.1	82.2	90.7	--	--
PGFL-KD [33]	87.2	95.3	79.5	89.6	--	--
AML [14]	89.5	95.7	81.7	91.1	82.3	85.6
PFD [30]	89.7	95.5	82.2	90.6	--	--
SOLIDER [3]	95.3	96.6	86.1	89.4	71.6	67.4
PGS-1	<u>95.4</u>	96.9	<u>90.0</u>	93.0	<u>83.5</u>	85.6
PGS-2	<u>95.4</u>	<u>97.1</u>	<u>90.0</u>	92.5	88.3	<u>86.5</u>
PGS-3	95.6	97.2	90.1	<u>92.7</u>	88.3	86.8

Table 1: Quantitative results on the clothes-consistent datasets. The highest and second highest scores are shown in **bold** and underline, respectively.

Method	LTCC-Standard		LTCC-CC		VC-Clothes	
	mAP	R1	mAP	R1	mAP	R1
LTCC [25]	34.3	71.4	11.7	25.2	--	--
FSAM [13]	35.4	73.2	16.2	38.5	<u>78.9</u>	78.6
CAL [9]	40.8	74.2	18.0	40.1	--	--
GI-ReID [15]	29.4	63.2	10.4	23.7	59.0	63.7
AIM [32]	41.1	76.3	19.1	40.6	74.1	73.7
FIRe ² [29]	39.9	75.9	19.1	44.6	--	--
PGS-1	42.7	<u>77.0</u>	<u>27.1</u>	67.8	78.6	90.4
PGS-2	<u>42.8</u>	<u>77.0</u>	<u>27.1</u>	<u>70.5</u>	78.6	<u>89.9</u>
PGS-3	43.0	77.5	27.2	72.5	79.1	90.4

Table 2: Quantitative results on LTCC dataset and the VC-Clothes dataset. The highest and second highest scores are shown in **bold** and underline, respectively.

Clothes-changing: From Table 2, our model demonstrates an improvement of over +1.9% in mAP and +1.2% in the R1 metric for standard testing. In the clothes-changing testing scenario, our method achieves a remarkable +6.1% improvement in mAP and surpasses the second-best by a substantial margin of +27.9%. Regarding the VC-Clothes dataset, our method surpasses the second by +0.2% in mAP and achieves a significant improvement by +11.8%. These results highlight the competitiveness of our method with state-of-the-art approaches to the VC-Clothes dataset. This improvement is attributed to our pose-guided approach, which enables the model to retain pose information while also focusing on the overall human shape, including features beyond clothing such as the body and arms.

	LTCC-Standard		LTCC-CC	
Method	mAP	R1	mAP	R1
PGS-1	42.7	<u>77.0</u>	<u>27.1</u>	67.8
PGS-2	<u>42.8</u>	<u>77.0</u>	<u>27.1</u>	<u>70.5</u>
PGS-3	43.0	77.5	27.2	72.5

Table 3: Impact of the pose guidance across multiple scales.

4.5 Ablation Studies

To evaluate the effectiveness of the PGS, we perform three studies: the first experiment evaluates the effectiveness of the pose guidance via multiple scales with the baseline (human encoder), the second experiment is the cross-domain testing to explore the generalization of the trained model, and the final experiment demonstrates the effectiveness of our TTK module.

Effect of supervision via multiple scales: Table 3 shows the evaluation of our framework, which is guided via multiple scales. We can observe the results of PGS-3 achieving the best in three versions, which illustrates the significant improvement when guidance occurs in multiple layers.

Cross-domain testing: To evaluate the generalization of our model, we perform the cross-domain testing with two experiments: Duke-MTMC (source) \rightarrow Market-1501 (target) and Market-1501 (source) \rightarrow Duke-MTMC (target). We compared our framework with several methods: SSL [23], ATNet [18], UDAP [24], and the baseline is the SOLIDER [3]. From Table 4, our model in three versions achieves competitive results in both cross-domain settings, which reflects the robustness of our model in cross-domain ReID.

	D \rightarrow M		M \rightarrow D	
Method	mAP	R1	mAP	R1
SSL [23]	37.8	71.7	28.6	52.5
ATNet [18]	25.6	55.7	24.9	45.1
UDAP [24]	53.7	<u>75.8</u>	49.0	<u>68.4</u>
SOLIDER [3]	50.3	59.9	50.3	59.9
PGS-1	57.7	73.3	52.3	61.7
PGS-2	<u>59.1</u>	76.4	<u>52.9</u>	62.1
PGS-3	61.6	76.4	53.6	72.7

Table 4: Results on the cross-domain testing. D, M represent the Duke-MTMC and Market-1501 dataset.

Effect of the TTK module: To assess the performance of the TTK module, we conducted experiments in two scenarios: the first case involved only the reduction stage as the transfer feature (i.e., w/o f_t), and the second case involved both reduction and transformation stages in our module (i.e., w f_t). In Table 5, the results show that integrating the Transformer feature (transformation stage) leads to better performance, demonstrating the effectiveness of integrating the

Method	LTCC standard		LTCC-CC	
	mAP	R1	mAP	R1
W/o f_{t-1}	41.1	76.1	26.3	65.5
W f_{t-1}	42.7	77.0	27.1	67.8
W/o f_{t-2}	42.0	75.9	26.5	66.7
W f_{t-2}	42.8	77.0	27.1	70.5
W/o f_{t-3}	41.1	75.5	26.3	65.8
W f_{t-3}	43.0	77.5	27.2	72.5

Table 5: Impact of the TTK module on the model’s performance.

Transformer layer into our TTK modules at multiple scales in both clothes-consistent and clothes-changing settings.

4.6 Feature Map Visualization

To further understand the behaviour of our trained model, we perform the heatmap visualization which can be seen in Figure 3. We can easily observe that the result heatmaps of three versions focus on the head of a human, on the body, and on other parts of the human’s body. In simpler terms, the combination of the human encoder, pose encoder, and the TTK module empowers the model to prioritize the human’s body accurately, mitigate the reliance on clothes.

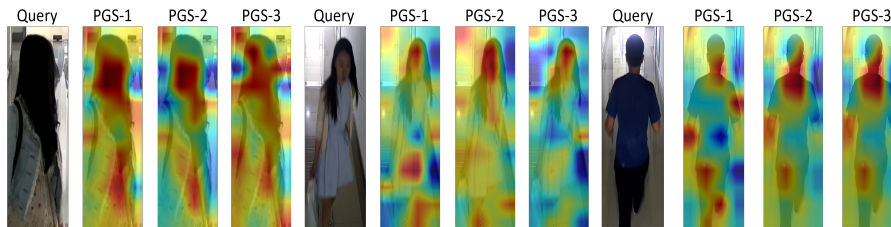


Fig. 3: The heatmap visualization to understand the behaviour of our framework.

5 Conclusion

In conclusion, this paper introduces the concept of Pose Guidance Supervision (PGS), which transfers the pose knowledge into the ReID model at multiple scales for robust ReID in scenarios involving both clothes-consistent and clothes-changing. Our study demonstrates the effectiveness of this approach in enabling the model to learn robust features, as evidenced by competitive results in comparison to state-of-the-art methods and improvements over the baseline, as indicated by ablation studies. This simple approach is a promising candidate for real-world camera surveillance applications and provides a solid foundation for future studies aimed at building more robust models. We encourage other researchers to explore multiple ways to extract the human representation as well as biometric traits to further enhance the performance of the ReID models.

References

1. Cao, Z., Hidalgo Martinez, G., Simon, T., Wei, S., Sheikh, Y.A.: Openpose: Real-time multi-person 2d pose estimation using part affinity fields. *IEEE Transactions on Pattern Analysis and Machine Intelligence* (2019)
2. Chen, T., Ding, S., Xie, J., Yuan, Y., Chen, W., Yang, Y., Ren, Z., Wang, Z.: Abd-net: Attentive but diverse person re-identification. In: *Proceedings of the IEEE/CVF International Conference on Computer Vision* (2019)
3. Chen, W., Xu, X., Jia, J., Luo, H., Wang, Y., Wang, F., Jin, R., Sun, X.: Beyond appearance: a semantic controllable self-supervised learning framework for human-centric visual tasks. In: *The IEEE/CVF Conference on Computer Vision and Pattern Recognition* (2023)
4. Dao, T.V., Dinh, T.B., Dinh, T.B.: Multi-branch network with dynamically matching algorithm in person re-identification. In: *2020 7th NAFOSTED Conference on Information and Computer Science (NICS)* (2020)
5. Dosovitskiy, A., Beyer, L., Kolesnikov, A., Weissenborn, D., Zhai, X., Unterthiner, T., Dehghani, M., Minderer, M., Heigold, G., Gelly, S., et al.: An image is worth 16x16 words: Transformers for image recognition at scale. *arXiv preprint arXiv:2010.11929* (2020)
6. Gao, S., Wang, J., Lu, H., Liu, Z.: Pose-guided visible part matching for occluded person reid. In: *Proceedings of the IEEE/CVF Conference on Computer Vision and Pattern Recognition* (2020)
7. Gong, Y., Wang, L., Cheng, S., Li, Y.: A strong baseline based on adaptive mining sample loss for person re-identification. In: *CAAI International Conference on Artificial Intelligence* (2021)
8. Gu, H., Fu, G., Li, J., Zhu, J.: Auto-reid+: Searching for a multi-branch convnet for person re-identification. *Neurocomputing* **435**, 53–66 (2021)
9. Gu, X., Chang, H., Ma, B., Bai, S., Shan, S., Chen, X.: Clothes-changing person re-identification with rgb modality only. In: *Proceedings of the IEEE/CVF Conference on Computer Vision and Pattern Recognition* (2022)
10. He, S., Luo, H., Wang, P., Wang, F., Li, H., Jiang, W.: Transreid: Transformer-based object re-identification. In: *Proceedings of the IEEE/CVF International Conference on Computer Vision* (2021)
11. Hermans, A., Beyer, L., Leibe, B.: In defense of the triplet loss for person re-identification. *arXiv preprint arXiv:1703.07737* (2017)
12. Hoffer, E., Ailon, N.: Deep metric learning using triplet network. In: *International Workshop on Similarity-Based Pattern Recognition*. pp. 84–92 (2015)
13. Hong, P., Wu, T., Wu, A., Han, X., Zheng, W.S.: Fine-grained shape-appearance mutual learning for cloth-changing person re-identification. In: *Proceedings of the IEEE/CVF Conference on Computer Vision and Pattern Recognition* (2021)
14. Huang, Z., Wang, L., Li, Y., Du, A., Jiang, S.: Improving performance in person reidentification using adaptive multiple loss baseline. *Information* **13**(10), 453 (2022)
15. Jin, X., He, T., Zheng, K., Yin, Z., Shen, X., Huang, Z., Feng, R., Huang, J., Chen, Z., Hua, X.S.: Cloth-changing person re-identification from a single image with gait prediction and regularization. In: *Proceedings of the IEEE/CVF Conference on Computer Vision and Pattern Recognition* (2022)
16. Li, J., Zhang, S., Tian, Q., Wang, M., Gao, W.: Pose-guided representation learning for person re-identification. *IEEE Transactions on Pattern Analysis and Machine Intelligence* **44**(2), 622–635 (2019)

17. Li, W., Zhao, R., Xiao, T., Wang, X.: Deepreid: Deep filter pairing neural network for person re-identification. In: Proceedings of the IEEE/CVF Conference on Computer Vision and Pattern Recognition (2014)
18. Liu, J., Zha, Z.J., Chen, D., Hong, R., Wang, M.: Adaptive transfer network for cross-domain person re-identification. In: Proceedings of the IEEE/CVF Conference on Computer Vision and Pattern Recognition (2019)
19. Liu, J., Ni, B., Yan, Y., Zhou, P., Cheng, S., Hu, J.: Pose transferrable person re-identification. In: Proceedings of the IEEE/CVF Conference on Computer Vision and Pattern Recognition (2018)
20. Liu, Z., Lin, Y., Cao, Y., Hu, H., Wei, Y., Zhang, Z., Lin, S., Guo, B.: Swin transformer: Hierarchical vision transformer using shifted windows. In: Proceedings of the IEEE/CVF International Conference on Computer Vision (2021)
21. Loshchilov, I., Hutter, F.: Decoupled weight decay regularization. arXiv preprint arXiv:1711.05101 (2017)
22. Luo, H., Gu, Y., Liao, X., Lai, S., Jiang, W.: Bag of tricks and a strong baseline for deep person re-identification. In: Proceedings of the IEEE/CVF Conference on Computer Vision and Pattern Recognition Workshops (2019)
23. Luo, H., Wang, P., Xu, Y., Ding, F., Zhou, Y., Wang, F., Li, H., Jin, R.: Self-supervised pre-training for transformer-based person re-identification. arXiv preprint arXiv:2111.12084 (2021)
24. Peng, P., Xiang, T., Wang, Y., Pontil, M., Gong, S., Huang, T., Tian, Y.: Unsupervised cross-dataset transfer learning for person re-identification. In: Proceedings of the IEEE/CVF Conference on Computer Vision and Pattern Recognition (2016)
25. Qian, X., Wang, W., Zhang, L., Zhu, F., Fu, Y., Xiang, T., Jiang, Y.G., Xue, X.: Long-term cloth-changing person re-identification. In: Proceedings of the Asian Conference on Computer Vision (2020)
26. Quan, R., Dong, X., Wu, Y., Zhu, L., Yang, Y.: Auto-reid: Searching for a part-aware convnet for person re-identification. In: Proceedings of the IEEE/CVF International Conference on Computer Vision (2019)
27. Ristani, E., Solera, F., Zou, R., Cucchiara, R., Tomasi, C.: Performance measures and a data set for multi-target, multi-camera tracking. In: European Conference on Computer Vision workshop on Benchmarking Multi-Target Tracking (2016)
28. Wan, F., Wu, Y., Qian, X., Chen, Y., Fu, Y.: When person re-identification meets changing clothes. In: Proceedings of the IEEE/CVF Conference on Computer Vision and Pattern Recognition Workshops (2020)
29. Wang, Q., Qian, X., Li, B., Fu, Y., Fu, Y., Xue, X.: Exploring fine-grained representation and recomposition for cloth-changing person re-identification. arXiv preprint arXiv:2308.10692 (2023)
30. Wang, T., Liu, H., Song, P., Guo, T., Shi, W.: Pose-guided feature disentangling for occluded person re-identification based on transformer. In: Proceedings of the AAAI Conference on Artificial Intelligence (2022)
31. Wu, Y., Lin, Y., Dong, X., Yan, Y., Ouyang, W., Yang, Y.: Exploit the unknown gradually: One-shot video-based person re-identification by stepwise learning. In: Proceedings of the IEEE/CVF Conference on Computer Vision and Pattern Recognition (2018)
32. Yang, Z., Lin, M., Zhong, X., Wu, Y., Wang, Z.: Good is bad: Causality inspired cloth-debiasing for cloth-changing person re-identification. In: Proceedings of the IEEE/CVF Conference on Computer Vision and Pattern Recognition (2023)
33. Zheng, K., Lan, C., Zeng, W., Liu, J., Zhang, Z., Zha, Z.J.: Pose-guided feature learning with knowledge distillation for occluded person re-identification. In: Proceedings of the 29th ACM International Conference on Multimedia (2021)

34. Zheng, L., Shen, L., Tian, L., Wang, S., Wang, J., Tian, Q.: Scalable person re-identification: A benchmark. In: Proceedings of the IEEE/CVF Conference on Computer Vision and Pattern Recognition (2015)
35. Zhong, Z., Zheng, L., Cao, D., Li, S.: Re-ranking person re-identification with k-reciprocal encoding. In: Proceedings of the IEEE/CVF Conference on Computer Vision and Pattern Recognition (2017)